Are granites and granulites consanguineous?

Fawna Korhonen[1], Michael Brown[2], Chris Clark[3], John D. Foden[4], and Richard Taylor[3]
[1]Geological Survey of Western Australia, East Perth, WA 6004, Australia
[2]Laboratory for Crustal Petrology, Department of Geology, University of Maryland, College Park, Maryland 20742, USA
[3]Department of Applied Geology, Curtin University, GPO Box U1987, Perth, WA 6845, Australia
[4]Department of Earth Sciences, University of Adelaide, Adelaide, SA 5005, Australia

ABSTRACT

An important question in petrology is whether the production of granite magma in orogens is a closed-system process with respect to mass input from the mantle. This is commonly addressed by inversion of geochemical data from upper crustal granites, but a complementary approach is to assess the kinship of residual granulites and associated granites in exhumed orogenic crust. Here we report geochemical data for a suite of contemporaneous metasedimentary granulites and granites from the Eastern Ghats Province, India, part of a Grenville-age orogen. The prograde metamorphic evolution involved increasing temperature (*T*) and pressure (*P*) to a metamorphic peak at >1000 °C at ~0.7 GPa, followed by slow close-to-isobaric cooling. Variations in the composition of granites are interpreted to be due to local processes, including fractionation during melting or crystallization, and/or peritectic mineral entrainment. The Nd and Sr isotope compositions of the granites can be matched by mixing between different granulites, suggesting that they may have been derived solely from sedimentary protoliths leaving behind granulite facies residues. However, by including geochemical data from an adjacent area to the north, it becomes clear that an increasingly important mass input from the mantle was involved in granite genesis from southwest to northeast in the Eastern Ghats Province, as confirmed by modeling assimilation–fractional crystallization between an exemplar mantle-derived melt at 1000 Ma and the residual granulites. The extreme peak metamorphic temperature and *P–T* evolution suggest extended lithosphere that relaxed thermally to its former thickness during slow cooling. We postulate that the spatial variation in mantle input to the granites was related to changing feedback between the rates of extension and flux of mantle melt.

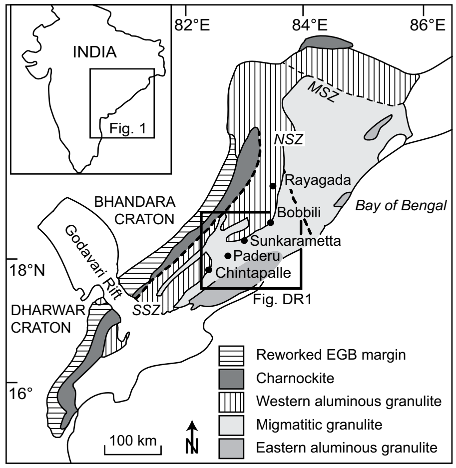

Figure 1. Eastern Ghats belt (EGB; India) and adjacent cratons, showing broad lithological associations and major shear zones bounding the Eastern Ghats Province. MSZ—Mahanadi shear zone; NSZ—Nagavalli shear zone; SSZ—Sileru shear zone.

INTRODUCTION

In active orogens, melt is generated in the middle to lower crust and imaged as sills and magma bodies in the middle to upper crust (Gaillard et al., 2004; del Potro et al., 2013). By contrast, exhumed granulites in ancient orogens represent residues from crustal anatexis after melt has drained away, so they provide insight into granite generation and the process of melt extraction complementary to studies of active orogens (Brown, 2013).

In one school of thought, the kinship between residual granulites and granites has been argued to be consanguineous—i.e., derived from common crustal protoliths (Vielzeuf et al., 1990; Korhonen et al., 2010). In an alternative view, it is posited that although residual granulites and granites have some features in common, the mantle has contributed mass to the crustal magmas (Smithies et al., 2011). The heat necessary to achieve granulite facies temperatures and drive extensive melting may be generated either by high concentrations of heat-producing elements and low erosion rates (Clark et al., 2011), via mantle-derived magmas emplaced at depth (Bohlen, 1991), or by a combination of these processes.

Because granite magmatism plays an important role in crustal reworking and differentiation (Michaut et al., 2009), it is important to determine whether any incursion of mantle heat to promote crustal melting also had an input of mass to the magmas. To assess whether granite generation was a closed- or open-system process with respect to the mantle, we undertook a geochemical study of granulites and spatially associated granites in exhumed lower crust from the Eastern Ghats Province, India. In addition to providing new data along a 130 km traverse, we include in the study data from an area to the north (Shaw et al., 1997) to ensure that any spatial variation in these processes is fully evaluated.

EASTERN GHATS, INDIA

The Eastern Ghats Province lies between the Godavari Rift in the south and the Nagavalli shear zone in the north within the Proterozoic Eastern Ghats belt (Fig. 1). The Eastern Ghats Province is dominated by aluminous granulite, inferred to be derived from pelite protoliths, and migmatitic granulite, inferred to be derived from a greywacke protolith (Fig. 1). The granulites preserve peak mineral assemblages without significant retrogression and have refractory chemical compositions (discussed below), consistent with them being residues after loss of granite melt. The prograde metamorphic evolution of increasing temperature (*T*) before pressure (*P*), reaching a peak at >1000 °C at ~0.7 GPa, was followed by slow close-to-isobaric cooling across an elevated solidus appropriate to these residual rocks (Korhonen et al., 2013b, 2014).

Samples

First, we briefly summarize relationships between samples of granulite and granite collected along a 130 km traverse from Bobbili in the northeast to Chintapalle in the southwest (Fig. 1, Fig. DR1 and Table DR1 in the GSA Data Repository[1]). In the northeast, near Bobbili, a foliated plagioclase-phyric biotite-garnet trondhjemite (sample 10-66) is associated with quartz-rich sillimanite-garnet granulite (samples 10-65, 10-67). To the east-southeast of Bobbili, the outcrops are dominated by migmatite composed of an orthopyroxene-garnet granulite (sample 09-52) that hosts both concordant (sample 10-61) garnet-bearing and discordant (sample 10-60) garnet ± orthopyroxene ± biotite–bearing leucosomes (Fig. DR2A). Close to Sunkarametta, K-feldspar-phyric orthopyroxene granite (sample 09-35) is associated with orthopyroxene-garnet granulite (sample 09-34). To the west of Paderu, biotite-garnet granite (sample 09-19) occurs in association with dominant orthopyroxene-garnet granulite (sample 09-01) and subordinate high-Mg granulite characterized by pseudomorphs after osumilite (samples 09-02, 09-04; Korhonen et al., 2013a). In the

[1]GSA Data Repository item 2015334, Figures DR1–DR6 and Tables DR1–DR4, is available online at www.geosociety.org/pubs/ft2015.htm, or on request from editing@geosociety.org or Documents Secretary, GSA, P.O. Box 9140, Boulder, CO 80301, USA.

GEOLOGY, November 2015; v. 43; no. 11; p. 991–994 | Data Repository item 2015334 | doi:10.1130/G37164.1 | Published online 1 October 2015

southwest, near Chintapalle, variably schlieric K-feldspar-phyric garnet-bearing leucogranite (samples 10-90, 10-92, 10-93; note that 10-93 has higher modal garnet) occurs in association with sillimanite-garnet-K-feldspar granulite (Fig. DR2B; samples 10-88, 10-91, 10-94).

GEOCHRONOLOGY AND GEOCHEMISTRY

Geochronology

We determined zircon and monazite U-Pb data for a migmatitic orthopyroxene-garnet granulite (sample 09-52) and an associated leucosome (10-61), and zircon U-Pb data for two sillimanite-garnet granulites (10-67 and 10-94) and associated granites (10-66 and 10-93) to assess contemporaneity with Grenville-age orogenesis. The analytical protocol and data are provided in the Data Repository (Tables DR2 and DR3) together with a discussion of the concordia plots, normalized rare earth element plots for zircon, and cathodoluminescence images of zircon and backscattered-electron images of monazite (Figs. DR3–DR5). These new data confirm that granulite facies metamorphism and crustal anatexis occurred during the interval 1000–900 Ma, consistent with the regional study of Korhonen et al. (2013b), who interpreted zircon and monazite ages of 980–930 Ma across the area to record post-peak cooling to an elevated solidus at a rate of ~1 °C/m.y.

Geochemistry

Chemical compositions of 18 samples were determined at Franklin and Marshall College (Pennsylvania, USA) by combining X-ray fluorescence spectroscopy, using a Phillips 2404 instrument, with loss on ignition and FeO determination by Fe^{2+} titration. The Nd and Sr isotope compositions were determined by thermal ionization mass spectrometry at the University of Adelaide (Australia) following the same protocol as Pankhurst et al. (2011). The analytical data are given in Table DR4.

The geochemistry of the granulites and granites is discussed in relation to exemplar pelite and greywacke compositions and melt compositions from widely cited fluid-absent melting experiments at appropriate *P*–*T* conditions. For pelite, we use two kyanite zone rocks that are a match to the likely source compositions of the Himalayan leucogranites, which are accepted as crystallized from crustal melts (Patiño Douce and Harris, 1998). For greywacke, we use the upper amphibolite facies biotite-plagioclase-quartz rock from the Massif Central (France) studied by Montel and Vielzeuf (1997), which is very close to average greywacke in composition.

Elemental Geochemistry

The sillimanite-garnet granulites have high Al_2O_3 and low ($Na_2O + CaO$) and Sr compared to the orthopyroxene-garnet granulites (Fig. 2; Fig. DR6); ($MgO + FeO + Fe_2O_3 + TiO_2$) generally decreases with increasing SiO_2, whereas K_2O contents are similar. The low SiO_2 and high ($MgO + FeO + Fe_2O_3 + TiO_2$) relative to the exemplar pelite and greywacke compositions are consistent with the granulites being partial melt residues.

For granites associated with the sillimanite-garnet granulites (Fig. 2), Al_2O_3 and ($MgO + FeO + Fe_2O_3 + TiO_2$) are lower and ($Na_2O + CaO$) is higher than in the local host granulite. K_2O and Rb/Sr are higher in the granites than in the granulites and generally increase with increasing SiO_2, except in one sample that is dominated by plagioclase rather than K-feldspar (sample 10-66), as reflected in the highest ($Na_2O + CaO$). Trace element concentrations are variable. The two granites with the highest SiO_2 and lowest ($MgO + FeO + Fe_2O_3 + TiO_2$) also have low La, Zr, Y, U, and Th (Fig. DR6). By contrast, granite 10-93, which has higher modal garnet than spatially related granites (10-90 and 10-92), has higher ($MgO + FeO + Fe_2O_3 + TiO_2$), La, Zr, Y, and Th (Fig. DR6). The granites do not have correlated La and P_2O_5, La and Th, or Zr and Y, suggesting no control by, or systematic variations in, modal apatite, monazite, or zircon contents.

For granites and leucosomes associated with the orthopyroxene-garnet granulites (Fig. 2), SiO_2 varies from ~64 to ~76 wt%, while Al_2O_3 and ($Na_2O + CaO$) are lower and ($MgO + FeO + Fe_2O_3 + TiO_2$), K_2O, and Rb/Sr vary compared to the local host granulite. Trace element concentrations are variable. For the two granites, one (sample 10-19) has high La, Zr, Y, U, and Th, whereas the other (09-35) has moderate La and Y and high Zr, but low U and Th (Fig. DR6). With increasing SiO_2 the two leucosomes show decreasing La, Zr, and Y and increasing U. The granites do not have correlated La and P_2O_5, La and Th, or Zr and Y, suggesting no control by, or

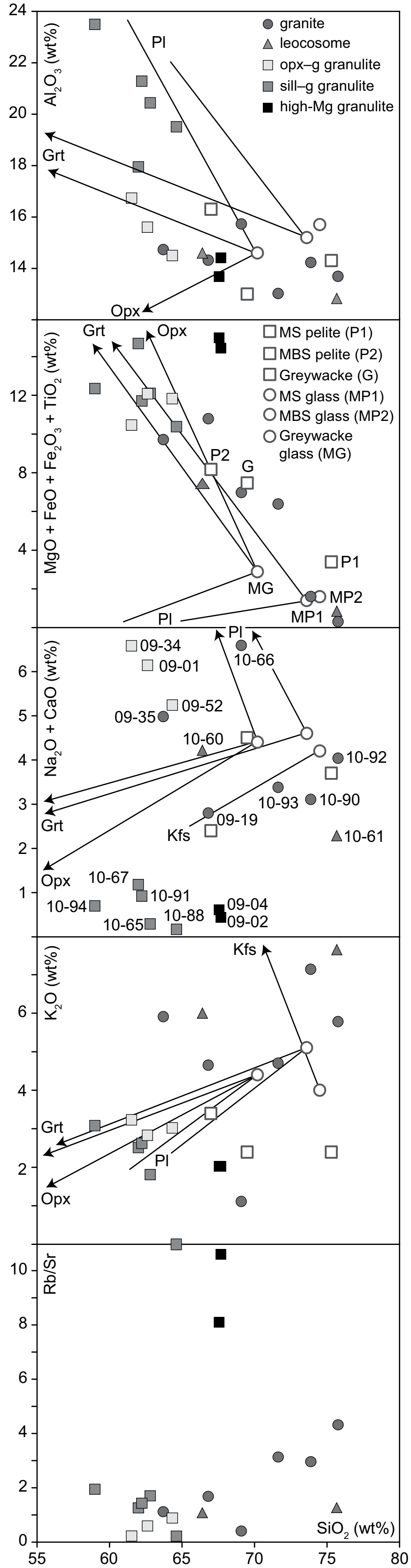

Figure 2. Select oxides and Rb/Sr versus SiO_2 for granulites and granites from Eastern Ghats Province (India). Also shown are muscovite schist (MS) and muscovite-biotite schist (MBS), and glass compositions (for MS, average of two compositions for temperature [*T*] = 900 °C at pressure [*P*] = 0.6 and 0.8 GPa [MP1]; for MBS, average of two compositions for *T* = 820 °C at *P* = 1.0 GPa [MP2]) from fluid-absent melting experiments of Patiño Douce and Harris (1998), greywacke and a glass composition (average of five compositions for *T* = 875–1040 °C at *P* = 0.8 GPa [MG]) from fluid-absent melting experiments of Montel and Vielzeuf (1997), and selected mineral fractionation vectors from both studies. Abbreviations in plots: Pl—plagioclase; Grt—garnet; Opx—orthopyroxene; Kfs—K-feldspar. Abbreviations in symbol explanation: opx—orthopyroxene; g—garnet; sill—sillimanite.

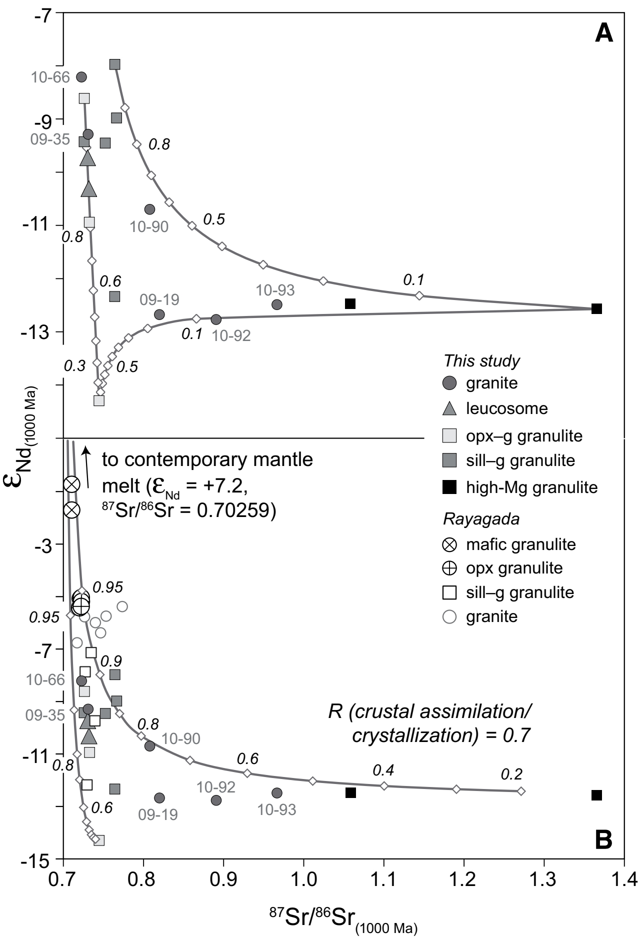

Figure 3. A. ε_{Nd} versus $^{87}Sr/^{86}Sr$ isotope compositions at 1000 Ma for granulites and granites from Eastern Ghats Province (India). Diamonds along binary mixing curve are at 10% increments. B. ε_{Nd} versus $^{87}Sr/^{86}Sr$ isotopic compositions at 1000 Ma for data in A and data for the Rayagada area in Shaw et al. (1997). Diamonds along assimilation–fractional crystallization mixing curves are at increments of 0.05, or 0.1 between 0.2 and 1. opx—orthopyroxene; g—garnet; sill—sillimanite.

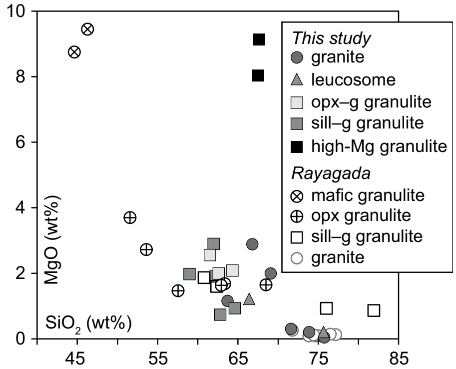

Figure 4. SiO_2 versus MgO for samples from this study (Eastern Ghats Province, India) and for mafic granulites, orthopyroxene granulites, and granites from the Rayagada area (Rajib Shaw, unpublished data not formally accepted for publication. Used with permission). opx—orthopyroxene; g—garnet; sill—sillimanite.

systematic variations in, modal apatite, monazite, or zircon contents.

Compositional variations in the granites are best explained as a consequence of processes such as fractionation during melting or crystallization and peritectic mineral entrainment acting locally, consistent with the granites being crystallized vestiges of draining melt. The concordant leucosome (sample 10-61) and the two leucogranites from the southwest of the study area (10-90 and 10-92) have compositions similar to those of experimental melts derived from the two typical pelite compositions, such as high SiO_2, low ($MgO + FeO + Fe_2O_3 + TiO_2$), high Rb/Sr, and low La, Zr, Y, U, and Th, but modified by plagioclase fractionation and K-feldspar accumulation (lower Na_2O + CaO and higher K_2O, respectively). By contrast, the discordant leucosome (10-60) and two of the granites (09-35 and 10-66) from the northeast of the study area have compositions consistent with accumulation of feldspar, such as high Na_2O + CaO, and for sample 09-35, high K_2O, high Sr, and moderate La and Y. Finally, several granites (09-19, 10-66, and 10-93) and the discordant leucosome (10-60) record evidence of peritectic mineral entrainment, particularly garnet ± orthopyroxene, as seen in the field and in thin section and as expressed by high ($MgO + FeO + Fe_2O_3 + TiO_2$) and, for samples 09-19 and 10-93, high Zr and Y.

Isotope Geochemistry

The Nd and Sr isotope compositions of the granulites and granites at 1000 Ma are variable (Fig. 3A), but most are relatively unradiogenic. However, four of the granites have higher $^{87}Sr/^{86}Sr$ and trend toward the two highly radiogenic high-Mg granulites which have $^{87}Sr/^{86}Sr$ of 1.058304 and 1.365787 respectively, consistent with the highest values from augen gneisses of the Indian basement under southern Tibet (Zeng et al., 2011). The depleted-mantle model age (T_{DM}) values range from 1.8 to 2.3 Ga (Table DR4), with one sillimanite-garnet granulite at 2.8 Ga, similar to the range of 1.8–2.9 Ga determined by Rickers et al. (2001) for the Eastern Ghats Province.

Binary mixing lines were calculated using the Nd and Sr concentrations and isotope values of more and less radiogenic end members of the granulite suite (Fig. 3A). These binary mixing lines enclose the Sr and Nd isotope values for all of the granulites, granites, and leucosomes of this study. The Sr and Nd isotope compositions of both leucosomes (samples 10-60 and 10-61) and granite 09-35 are consistent with derivation by partial melting from orthopyroxene-garnet granulite. However, the Sr and Nd isotope compositions of four of the other five granites (09-19, 10-90, 10-92, and 10-93) require a mixed source comprising orthopyroxene-garnet granulite and/or sillimanite-garnet granulite with high-Mg granulite in variable proportions (Fig. 3A). The trondhjemite (10-66) has the highest ε_{Nd} and appears to require an additional source component with more radiogenic Nd and relatively unradiogenic Sr.

In a wider context, in Figure 3B we include data from the study of Shaw et al. (1997) from an area near Rayagada, to the north of Bobbili (Fig. 1), where up to kilometer-scale bodies of leucogranite intrude sillimanite-garnet granulites, orthopyroxene granulites, and mafic granulites. In particular, the Nd and Sr isotope data for the mafic granulites, orthopyroxene granulites, and granites have significantly more radiogenic Nd but similarly non-radiogenic Sr isotope compositions compared to the new data from granulites and granites further southwest reported here (Fig. 3B). The extended data set defines a coupled trend of increasingly primitive (mantle-like) isotope compositions with decreasing whole-rock SiO_2 and increasing MgO (Fig. 4). These relationships, particularly the large changes in major element compositions, are typical of assimilation–fractional crystallization (AFC) between crust-like and mantle-like end-member components.

AFC Modeling

Figure 3B shows modeled AFC trends produced by interaction between an exemplar mantle-derived melt (average mid-oceanic ridge basalt, assuming an asthenospheric source appropriate to extended lithosphere, using trace element concentrations from Jenner and O'Neill [2012] and present-day $^{143}Nd/^{144}Nd$ = 0.513108 and $^{87}Sr/^{86}Sr$ = 0.702900, corrected back to 1000 Ma) and the range of crustal lithologies represented by orthopyroxene-garnet and sillimanite-garnet granulites (higher Sr) and Mg-rich granulites (lower Sr). In such models, the Nd/Sr of the radiogenic crustal end member controls the curvature of the mixing line (DePaolo, 1981). An AFC process could simultaneously explain the entire array of granulite and granite compositions, which range from dominantly crustal melts around Chintapalle and Paderu in the southwest (Fig. 3, samples 10-93, 10-92, 10-19, and 10-90) to those with an increasing mantle component to the northeast (Fig. 3, samples 09-35 and 10-66 and the Rayagada granites). Granites that plot to higher values of $^{87}Sr/^{86}Sr$ than the more radiogenic of the two modeled AFC trends may be explained if their original Rb/Sr has been modified by alteration, which affects the age-corrected $^{87}Sr/^{86}Sr$, or if the Nd/Sr value chosen for the radiogenic crustal end member was not appropriate along the extended traverse from Chintapalle to Rayagada (185 km).

DISCUSSION

When viewed in isolation, the new data presented herein permit derivation of the granites in the southern Eastern Ghats Province by mixing among anatectic melts derived from the regionally distributed granulites. However, when viewed in a wider context by including data from an area to the north, it becomes clear that mass input from the mantle is required to explain the expanded range of Nd isotope compositions. We envisage this suite of granulites and granites to have formed as a consequence of increasing open-system interaction from southwest to northeast between mantle-derived melts and suprasolidus metasedimentary rocks in the lower crust of an ultrahot orogen, similar to the process described for the genesis of S-type granites by Foden et al. (2015). The ultrahigh temperatures recorded regionally likely require an incursion of heat from the mantle, and the metamorphic evolution of thickening after heating suggests an extended lithosphere that relaxed thermally to its former thickness during slow cooling.

In this tectonic context, we postulate that the southwest-to-northeast spatial variation in mantle contribution to the granites was related to the changing feedback between rates of extension and mantle melt flux from southwest to northeast (cf. Karakas and Dufek, 2015). This process allowed the preservation of refractory granulite with remnants of crustal-sourced granite in the southwest, but to the northeast produced granites that require the involvement of an increasingly higher proportion of mantle melt in their genesis. This outcome is consistent with earlier speculation that crustal growth in the Eastern Ghats during Grenvillian orogenesis might have occurred in a northeast direction (Rickers et al., 2001).

In conclusion, we have used a combination of data to show that granites in the southwest of the Eastern Ghats Province are consanguineous with their regional granulite-facies residues, whereas those to the northeast require a significant mass input from the mantle. Thus, in the Eastern Ghats Province the granites in the southwest represent one end of a continuum in which there is a gradient in mantle contribution to granite magmas to the northeast as the granulite–granite kinship evolves from consanguineous to affinal.

ACKNOWLEDGMENTS

We thank Makoto Arima for assistance with data from the Rayagada area and Rajib Shaw for permission to use unpublished geochemical data from his Ph.D. thesis. We acknowledge constructive comments from Martin Streck, Mike Williams, and several anonymous reviewers, and helpful editorial advice from Brendan Murphy.

REFERENCES CITED

Bohlen, S.R., 1991, On the formation of granulites: Journal of Metamorphic Geology, v. 9, p. 223–229, doi:10.1111/j.1525-1314.1991.tb00518.x.

Brown, M., 2013, Granite: From genesis to emplacement: Geological Society of America Bulletin, v. 125, p. 1079–1113, doi:10.1130/B30877.1.

Clark, C., Fitzsimons, I.C.W., Healy, D., and Harley, S.L., 2011, How does the continental crust get really hot?: Elements (Quebec), v. 7, p. 235–240, doi:10.2113/gselements.7.4.235.

del Potro, R., Díez, M., Blundy, J., Camacho, A.G., and Gottsmann, J., 2013, Diapiric ascent of silicic magma beneath the Bolivian Altiplano: Geophysical Research Letters, v. 40, p. 2044–2048, doi:10.1002/grl.50493.

DePaolo, D.J., 1981, Trace element and isotopic effects of combined wallrock assimilation and fractional crystallization: Earth and Planetary Science Letters, v. 53, p. 189–202, doi:10.1016/0012-821X(81)90153-9.

Foden, J.D., Sossi, P.A., and Wawryk, C.M., 2015, Fe isotopes and the contrasting petrogenesis of A-, I- and S-type granite: Lithos, v. 212–215, p. 32–44, doi:10.1016/j.lithos.2014.10.015.

Gaillard, F., Scaillet, B., and Pichavant, M., 2004, Evidence for present-day leucogranite pluton growth in Tibet: Geology, v. 32, p. 801–804, doi:10.1130/G20577.1.

Jenner, F.E., and O'Neill, H.St.C., 2012, Major and trace analysis of basaltic glasses by laser-ablation ICP-MS: Geochemistry Geophysics Geosystems, v. 13, Q03003, doi:10.1029/2011GC003890.

Karakas, O., and Dufek, J., 2015, Melt evolution and residence in expending crust: Thermal modeling of the crust and crustal magmas: Earth and Planetary Science Letters, v. 425, p. 131–144, doi:10.1016/j.epsl.2015.06.001.

Korhonen, F.J., Saito, S., Brown, M., and Siddoway, C.S., 2010, Multiple generations of granite in the Fosdick Mountains, Marie Byrd Land, West Antarctica: Implications for polyphase intracrustal differentiation in a continental margin setting: Journal of Petrology, v. 51, p. 627–670, doi:10.1093/petrology/egp093.

Korhonen, F.J., Brown, M., Clark, C., and Bhattacharya, S., 2013a, Osumilite-bearing equilibria and implications for the evolution of the Eastern Ghats Province, India: Journal of Metamorphic Geology, v. 31, p. 881–907, doi:10.1111/jmg.12049.

Korhonen, F.J., Clark, C., Brown, M., Bhattacharya, S., and Taylor, R., 2013b, How long-lived is ultrahigh temperature (UHT) metamorphism? Constraints from zircon and monazite geochronology in the Eastern Ghats orogenic belt, India: Precambrian Research, v. 234, p. 322–350, doi:10.1016/j.precamres.2012.12.001.

Korhonen, F.J., Clark, C., Brown, M., and Taylor, R., 2014, Taking the temperature of Earth's hottest crust: Earth and Planetary Science Letters, v. 408, p. 341–354, doi:10.1016/j.epsl.2014.10.028.

Michaut, C., Jaupart, C., and Mareschal, J.-C., 2009, Thermal evolution of cratonic roots: Lithos, v. 109, p. 47–60, doi:10.1016/j.lithos.2008.05.008.

Montel, J.-M., and Vielzeuf, D., 1997, Partial melting of metagreywackes, Part II. Compositions of minerals and melts: Contributions to Mineralogy and Petrology, v. 128, p. 176–196, doi:10.1007/s004100050302.

Pankhurst, M.J., Vernon, R.H., Turner, S.P., Schaefer, B.F., and Foden, J.D., 2011, Contrasting Sr and Nd isotopic behaviour during magma mingling: New insights from the Mannum A-type granite: Lithos, v. 126, p. 135–146, doi:10.1016/j.lithos.2011.07.005.

Patiño Douce, A.E., and Harris, N., 1998, Experimental constraints on Himalayan anatexis: Journal of Petrology, v. 39, p. 689–710, doi:10.1093/petroj/39.4.689.

Rickers, K., Mezger, K., and Raith, M.M., 2001, Evolution of the continental crust in the Proterozoic Eastern Ghats Belt, and new constraints for Rodinia reconstruction: Implications from Sm–Nd, Rb–Sr and Pb–Pb isotopes: Precambrian Research, v. 112, p. 183–210, doi:10.1016/S0301-9268(01)00146-2.

Shaw, R.K., Arima, M., Kagami, H., Fanning, C.A.M., Shiraishi, K., and Motoyoshi, Y., 1997, Proterozoic events in the Eastern Ghats Granulite Belt, India: Evidence from Rb-Sr, Sm-Nd systematics, and SHRIMP dating: The Journal of Geology, v. 105, p. 645–656, doi:10.1086/515968.

Smithies, R.H., Howard, H.M., Evins, P.M., Kirkland, C.L., Kelsey, D.E., Hand, M., Wingate, M.T.D., Collins, A.S., and Belousova, E., 2011, High-temperature granite magmatism, crust mantle interaction and the Mesoproterozoic intracontinental evolution of the Musgrave Province, central Australia: Journal of Petrology, v. 52, p. 931–958, doi:10.1093/petrology/egr010.

Vielzeuf, D., Clemens, J.D., Pin, C., and Moinet, E., 1990, Granites, granulites, and crustal differentiation, *in* Vielzeuf, D., and Vidal, P., eds., Granulites and Crustal Evolution: Dordrecht, Netherlands, Kluwer Academic Publishers, NATO Advanced Science Institutes Series, Series C, Mathematical and Physical Sciences, v. 311, p. 59–85.

Zeng, L., Gao, L., Xie, K., and Liu-Zeng, J., 2011, Mid-Eocene high Sr/Y granites in the Northern Himalayan Gneiss Domes: Melting thickened lower continental crust: Earth and Planetary Science Letters, v. 303, p. 251–266, doi:10.1016/j.epsl.2011.01.005.

Manuscript received 16 July 2015
Revised manuscript received 8 September 2015
Manuscript accepted 11 September 2015

Printed in USA